



Thermal Performance Benchmarking

Annual Progress Report

Xuhui Feng

**NREL is a national laboratory of the U.S. Department of Energy
Office of Energy Efficiency & Renewable Energy
Operated by the Alliance for Sustainable Energy, LLC**

This report is available at no cost from the National Renewable Energy Laboratory (NREL) at www.nrel.gov/publications.

Management Report
NREL/MP-5400-67118
October 2017

Contract No. DE-AC36-08GO28308



Thermal Performance Benchmarking

Annual Progress Report

Xuhui Feng

**NREL is a national laboratory of the U.S. Department of Energy
Office of Energy Efficiency & Renewable Energy
Operated by the Alliance for Sustainable Energy, LLC**

This report is available at no cost from the National Renewable Energy Laboratory (NREL) at www.nrel.gov/publications.

National Renewable Energy Laboratory
15013 Denver West Parkway
Golden, CO 80401
303-275-3000 • www.nrel.gov

Management Report
NREL/MP-5400-67118
October 2017

Contract No. DE-AC36-08GO28308

NOTICE

This report was prepared as an account of work sponsored by an agency of the United States government. Neither the United States government nor any agency thereof, nor any of their employees, makes any warranty, express or implied, or assumes any legal liability or responsibility for the accuracy, completeness, or usefulness of any information, apparatus, product, or process disclosed, or represents that its use would not infringe privately owned rights. Reference herein to any specific commercial product, process, or service by trade name, trademark, manufacturer, or otherwise does not necessarily constitute or imply its endorsement, recommendation, or favoring by the United States government or any agency thereof. The views and opinions of authors expressed herein do not necessarily state or reflect those of the United States government or any agency thereof.

Cover Photos by Dennis Schroeder: (left to right) NREL 26173, NREL 18302, NREL 19758, NREL 29642, NREL 19795.

NREL prints on paper that contains recycled content.

Thermal Performance Benchmarking

Principal Investigator: Xuhui Feng

National Renewable Energy Laboratory
Transportation and Hydrogen Systems Center
15013 Denver West Parkway
Golden, CO 80401
Phone: (303) 275-4439
E-mail: xuhui.feng@nrel.gov

DOE Technology Development Manager: Susan A. Rogers

U.S. Department of Energy
1000 Independence Ave. SW EE-3V
Washington, DC 20585
Phone: 202-586-8997
E-mail: susan.rogers@ee.doe.gov

NREL Task Leader: Sreekant Narumanchi

Phone: 303-275-4062
Email: sreekant.narumanchi@nrel.gov

Contractor:
Contract No.:

Abstract/Executive Summary

The goal for this project is to thoroughly characterize the performance of state-of-the-art (SOA) in-production automotive power electronics and electric motor thermal management systems. Information obtained from these studies will be used to:

- Evaluate advantages and disadvantages of different thermal management strategies
- Establish baseline metrics for the thermal management systems
- Identify methods of improvement to advance the SOA
- Increase the publicly available information related to automotive traction-drive thermal management systems
- Help guide future electric-drive technologies (EDT) research and development efforts.

The performance results combined with component efficiency and heat generation information obtained by Oak Ridge National Laboratory (ORNL) may then be used to determine the operating temperatures for the EDT components under drive-cycle conditions. In FY16, the 2014 Honda Accord Hybrid power electronics thermal management system was benchmarked. Characterization of the 2015 BMW i3 power electronics thermal management system started in FY16, and the results will be reported in FY17.

The focus of this project is to benchmark the thermal aspects of the power electronics system. ORNL's benchmarking reports of electric and hybrid electric vehicle technology provide detailed descriptions of the electrical and packaging aspects of these automotive systems [1, 2].

Accomplishments

- We experimentally characterized the thermal performance of the 2014 Honda Accord Hybrid power electronics thermal management systems.

- We developed and validated both steady-state and transient thermal models of the 2014 Honda Accord power electronics systems. The models were used to identify the thermal bottlenecks within each system. Solutions to improve the thermal performance were proposed.
- We compared the thermal performance of the 2014 Honda Accord power electronics and 2012 Nissan LEAF power electronics systems to understand the advantage and disadvantage of different designs from cost and performance perspectives.
- We are working to understand heat loss distributions within each system. Heat loss information will be used as inputs into the transient models and used to compute component temperatures under drive-cycle operations.
- We initiated benchmarking of the 2015 BMW i3 power electronics and electric motor thermal management systems and completed the experimental measurements of the power electronics system.



Introduction

This project will seek out SOA power electronics and electric motor technologies to benchmark their thermal performance. Benchmarking will focus on the thermal aspects of the system. System metrics, including the junction-to-liquid thermal resistance, winding-to-liquid thermal resistance, and the parasitic power consumption of the heat exchangers, will be measured. The type of heat exchanger (i.e., channel flow, brazed, folded-fin) and any enhancement features will be identified and evaluated to understand their effect on performance. Additionally, the thermal resistance/conductivity of select power module and motor components will also be measured. The research conducted will allow insight into the various cooling strategies to understand which heat exchangers are most effective in terms of thermal performance and efficiency. Modeling analysis will also be carried out to better understand the heat transfer and fluid dynamics of the systems. The research conducted will allow insight into the various cooling strategies to understand the current SOA in thermal management for automotive power electronics and electric motors.

Approach

Hardware testing and modeling analyses were conducted to benchmark the performance of the power electronics and electric motor thermal management systems. The project approach is outlined below.

- Collaborate with industry and ORNL to identify the vehicle system to benchmark
 - The 2014 Honda Accord Hybrid power electronics thermal management system was benchmarked in FY16. Tests were initiated to measure the thermal performance of the 2015 BMW i3 power electronics thermal management system.
- Experimentally measure the performance of the thermal management systems
 - Measure the power electronics junction-to-liquid thermal resistances
 - Measure the thermal properties of the system components (e.g., thermal pads, stator laminations, motor windings)
 - Measure heat exchanger thermal resistance, pressure drop, volume, and weight.
- Create thermal models of the thermal management systems
 - Validate the models using experimental results
 - Compute thermal resistances that cannot be experimentally measured
 - Create transient thermal models and use them to estimate component temperatures under various drive-cycles.
- Analyze and report data
 - Identify thermal bottlenecks in the system and provide solutions to improve the SOA
 - Establish baseline metrics for the thermal management systems
 - Share results with industry and research institutions

- Support other EDT projects (power electronics thermal management research, electric motor thermal management research, benchmarking electric vehicle and hybrid electric vehicle technologies [ORNL]).

Results and Discussion

In FY16, the 2014 Honda Accord Hybrid power electronics thermal management systems were benchmarked. Experimental testing of the hardware was first completed to measure thermal resistance values of the systems. The laboratory tests were intended to provide an accurate means of measuring thermal performance of the systems and were not intended to simulate actual automotive operating conditions. Steady-state and transient models were then created and validated against the experimental data. The validated thermal models were used to further understand the heat transfer mechanisms within the systems. The goal is to use the models to compute component temperatures under drive-cycle conditions. Efforts to benchmark the 2015 BMW i3 power electronics thermal management system also started in FY16.

2014 Honda Accord Power Electronics (Inverter) Thermal Management System

Figure 1 shows pictures of the Honda Accord power electronics and cooling system. The Accord power electronics system consists of two inverters for the two electric machines (motor and generator) in the vehicle and one DC-to-DC boost converter. The Accord inverter does not use a “brick” style power module design, but instead uses a number of insulated gate bipolar transistor (IGBTs) and diodes soldered onto a direct-bond copper (DBC) substrate to create the two inverters and boost converter. The same size (footprint) IGBTs and diodes are used throughout the entire system [3]. It is also shown in Figure 1 that intricate finned structures are fabricated on the cold plate surface to augment cooling. Figure 2 shows the power module model created using a computer-aided-design (CAD) tool, and the cross-sectional view of the stack module structure (thermal path) of the Accord. Unlike the 2012 LEAF, the Accord does not utilize grease as a thermal interface material (TIM) between the layers, but still uses the conventional metalized-ceramic substrate.



Figure I-1: Pictures of the 2014 Honda Accord inverter. The left image shows the entire power electronics system and the middle image presents the cold plate cooling channels. The image on the right shows the intricate fins directly fabricated on the cold plate.

Photo Credit: Gilbert Moreno (NREL)

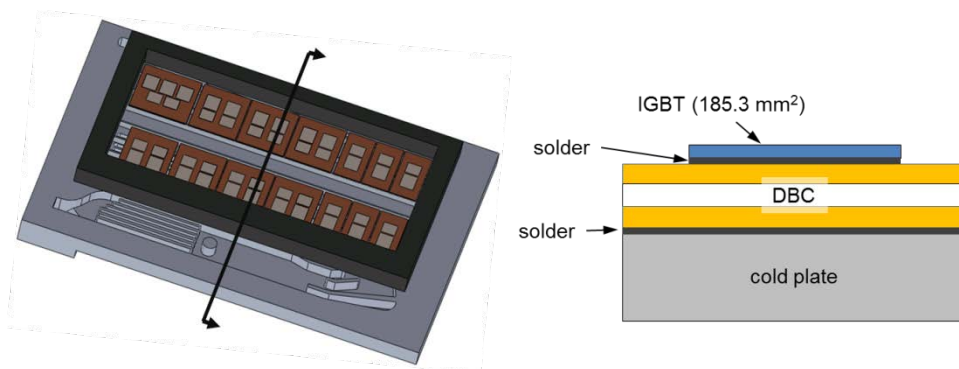


Figure I-2: CAD model of the Honda Accord power module (left). The various power module layers are shown in the cross-section view on the right.

Experiments were conducted to measure the junction-to-liquid resistance of the power modules. For the experiments, the module was connected to the water-ethylene glycol (WEG) flow test bench. The test bench circulated WEG (50%/50% water and ethylene glycol by volume) at a 65°C inlet temperature through the inverter cold plate at various flow rates. The experiments were repeated to ensure repeatable results. A transient thermal tester (T3ster) system was used to power/heat and measure the temperature of one IGBT. A total of 50 A were provided to power one IGBT (approximately 55 W of heat). Measuring temperatures required calibrating the voltage drop through the IGBT to its temperature. Temperature calibration was carried out within a temperature-controlled chamber. Two calibrated K-type thermocouples were mounted onto the power modules (placed near the IGBT that was to be tested) and used to obtain the temperature versus IGBT voltage drop relationship while supplying a 1-milliamp sense current through the device. Ten volts were used to gate the IGBT. The entire system was insulated with thick layers of insulation to minimize thermal losses to the surrounding environment. Then the specific thermal resistance was defined per Equation 1:

$$R''_{th, j-l} = \frac{(\bar{T}_j - \bar{T}_l)}{Q_{IGBT}} \times A_{IGBT} \quad \text{Equation 1}$$

where \bar{T}_j is the average junction temperature, \bar{T}_l is the average WEG temperature, Q_{IGBT} is the total heat dissipated through the IGBT, and A_{IGBT} is the area of the IGBT. Following the experimental procedure, the thermal performance of the 2014 Honda Accord power electronics system was characterized. Figure 3 shows the junction-to-liquid specific thermal resistance values at various flow rates. The 2014 Accord system provides thermal resistance values that are lower than the values from the 2012 Nissan LEAF that was characterized in FY15. The results also indicate that the passive stack thermal resistance is significantly larger than convective resistance (at the flow rates tested). At the typical automotive power electronic flow rates (~10 Lpm), the junction-to-liquid specific thermal resistance is about 44 mm²·K/W, nearly 50% lower than that of the Nissan LEAF. The Accord's lack of TIM layers is the likely reason for its superior thermal performance. The lack of a TIM layer in the Accord reduces its passive-stack thermal resistance, which makes it more sensitive to increasing convective heat transfer (i.e., increasing flow rates) as compared with the LEAF.

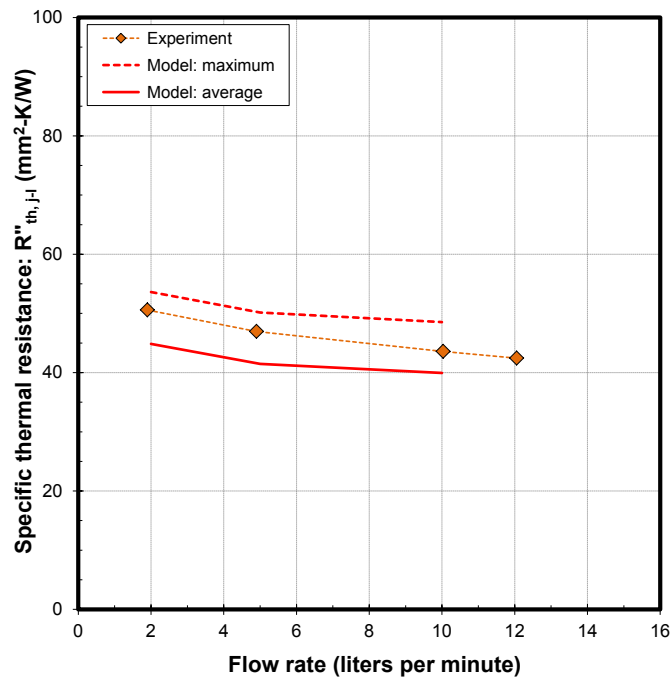


Figure I-3: Experimentally measured and model-predicted IGBT thermal resistance values for the 2014 Honda Accord inverter.

The laboratory tests were intended to provide an accurate means of measuring thermal resistance of power electronics systems and were not intended to simulate actual automotive operating conditions or environments. The experimental results were used to validate the thermal models which were then to be utilized to understand the thermal performance of the systems under various working conditions. Both computational fluid dynamics

(CFD) and finite element analysis (FEA) were applied to simulate the Accord power electronics thermal management systems to better understand the heat transfer within inverter. Table 1 lists the properties of the various power module components that were used in the models. Temperature-dependent thermal conductivity properties were used for silicon and copper. The thermal conductivities of the other components were obtained from literature. CFD-computed wetted-surface average heat transfer coefficients at various flow rates are provided in Table 2. The streamlines of the liquid and also the temperature profile on the cold plate surface calculated from the CFD simulation are presented in Figure 4. In the left graph of Figure 4, it clearly shows that the coolant flows through the finned structure and the temperature profile in the right graph also suggests where the hot spot locates.

The computed heat transfer coefficient values were imposed as boundary conditions in the FEA model. The FEA model replicated the experimental conditions (dissipate approximately 55 W through one IGBT). Once the models were validated by the experimental results, they are then applied to predict the steady-state and transient thermal resistance values under various conditions. The transient thermal resistance or thermal impedance (Z''_{th}) was computed using Equation 2.

$$Z''_{th, j-f} = \frac{(T_{j,max}(t) - T_f)}{Q_{IGBT}} \times A_{IGBT} \quad \text{Equation 2}$$

where $T_{j,max}(t)$ is the maximum junction temperature, T_f is the WEG temperature, Q_{IGBT} is the total heat dissipated through the IGBT, A_{IGBT} is the area of the IGBT, and t is time.

Figure 3 also provides the model-estimated maximum (computed using the maximum junction temperature) and average (computed using the average junction temperature) thermal resistance values. As shown, the model-predicted results provide a good match with the experimental data (maximum ~6% difference between model and experimental results). The FEA model was then used to generate a temperature profile from the IGBT to the liquid to identify the largest thermal bottlenecks in the system, with about 100 W of heat generated on the IGBT. The temperature profile is shown in Figure 5 and clearly shows that the passive stack provides the largest thermal bottleneck within the system. The silicon nitride layer is found to provide the largest resistance within the passive stack.

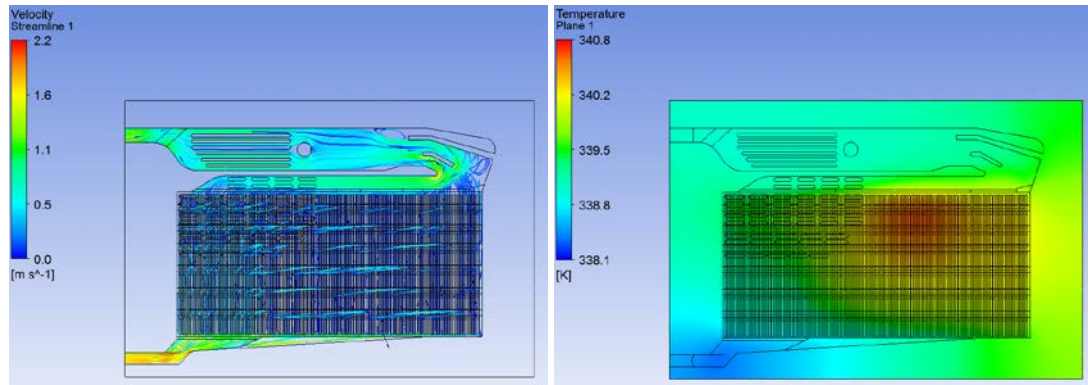


Figure I-4: CFD-generated plot showing the liquid velocity streamlines at a flow rate of 10 Lpm (left image) and the temperature distribution (right image) on the cold plate surface.

Table I-1: Thermal conductivity and thickness values used in the Honda Accord inverter thermal models

	Silicon [4]	Copper [4]	Silicon Nitride [5]	Aluminum [6]	Molding plastic [7]
--	-------------	------------	---------------------	--------------	---------------------

Thermal conductivity (W/m·K)	Temperature-dependent	Temperature-dependent	20	200	0.34
------------------------------	-----------------------	-----------------------	----	-----	------

Table I-2: CFD-predicted average heat transfer coefficient values for the Honda Accord inverter cold plate

Flow rate (Lpm)	Heat transfer coefficient (W/m ² ·K)
2.0	992
5.1	1793
9.8	2518

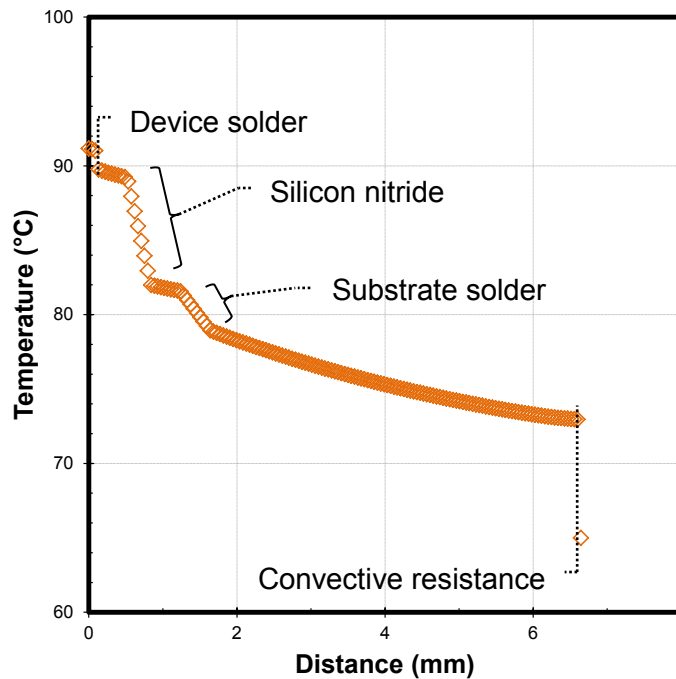


Figure I-5: Temperature profile through the Accord inverter depicting the thermal path from the IGBT to the liquid. The silicon nitride layer constitutes a significant thermal resistance in the power modules.

With the validated FEA model, simulations were conducted to analyze the steady-state thermal resistance of various power modules at a wide range of convective thermal resistance values (i.e., convective heat transfer coefficient values). The thermal performances of the LEAF and Accord systems were compared with the performance of a more conventional module design, which uses a metalized-ceramic substrate and a TIM layer between the module and the cold plate. Two conventional power module designs were studied. One design was achieved by replacing the copper-molybdenum plates and the dielectric pad with a DBC substrate. The DBC substrate has an alumina sheet of 0.38-mm thickness and two 0.25-mm-thick copper layers on both sides. The second conventional design was a Semikron SKM power module that also has an alumina DBC substrate. In both designs, a TIM layer is applied between the modules and an aluminum cold plate.

In the FEA models used to simulate the power module systems, only one power module was modeled and a three-to-one (IGBT-to-diode) heat loss ratio was used in the simulations. Because the Accord's power electronics does not use brick-type module design, only one half-bridge segment that consisted of two IGBT-diode pairs per switch was studied. The total power dissipated through the modules was adjusted so that the maximum junction temperatures reach 200°C, which is high for typical silicon-based devices. However, the 200°C junction temperature was applied here to simulate the high-temperature wide-bandgap devices. The liquid temperature was set to be 70°C. In these analyses, the finned structures on the cold plate surface were not modeled, and the convective thermal resistance was applied as a heat transfer coefficient boundary condition on the lower surface of the cold plate.

Figure 6 shows the specific thermal resistance versus the convective thermal resistance for the four power module systems introduced above. The thermal resistance was calculated using Equation 1 by applying the maximum junction temperature for \bar{T}_j . As presented in Figure 6, the LEAF (standard) power module has greater specific thermal resistance than that of the DBC-modified LEAF module. At 100 mm²·K/W convective thermal resistance, the Accord module's thermal resistance is about 38% and 12% lower than the LEAF and DBC-modified LEAF power modules, respectively. In addition, the Accord's module thermal resistance decreases at a faster rate with decreasing convective thermal resistance. This indicates that the Accord module has the lowest stack thermal resistance among the four systems characterized. It needs to be pointed out that the cooled surface area where the convective boundary condition is applied is different for the four designs and is the smallest for the Accord power module.

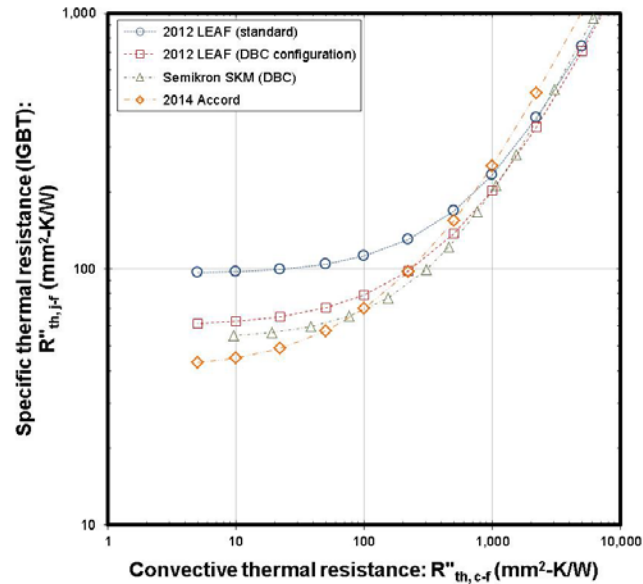


Figure I-6: Specific (junction-to-liquid) thermal resistance versus the convective thermal resistance for the standard LEAF, DBC-modified LEAF, the Accord, and Semikron modules. The Semikron data were from Bennion and Moreno [8].

FEA simulations were also conducted to study the transient thermal performance of three power modules. In Figure 7, the thermal impedances of the LEAF, DBC-modified LEAF and the Accord are shown. In the study, the power modules were initially at a uniform temperature of 70°C, and power to the devices was turned on (i.e., increasing temperature condition). The total heat applied on the power modules was 2,084 W, 2,956 W, and 1,865 W for the LEAF, DBC-modified LEAF, and Accord, respectively. The total heat was adjusted so that the maximum junction temperature reaches 200°C. Although the Accord has the lowest thermal resistance, it also has fewer IGBTs as compared to other modules and thus it dissipated the least amount of heat. A three-to-one IGBT-to-diode heat loss ratio and a convective thermal resistance of 100 mm²·K/W were applied in the simulation.

The impedance of the standard LEAF power module was found to be the lowest at a time of less than one second. This is probably due to the placement of a highly conductive copper-molybdenum plate directly below the IGBT and moving the low thermally conductive layer farther away from the IGBT-diode pair. In contrast, the DBC-modified LEAF module has a relatively low thermally conductive DBC plate close to the heat source, which limits the initial heat transfer. Additionally, the thermal mass of the copper-molybdenum layer

increases the heat capacitance near the devices. When the time is larger than one second, the thermal impedance of the standard LEAF becomes larger than that of the DBC-modified LEAF and the Accord modules, as it gradually approaches steady state. These trends indicate that the standard LEAF configuration may offer an advantage at transient conditions. Compared with the Accord power module design, the LEAF system also shows cost and reliability advantages. In the LEAF system, dielectric pads were used for insulation instead of metalized-ceramic substrates and the modules were directly mounted onto cast-aluminum cold plates instead of precesely machines plates.

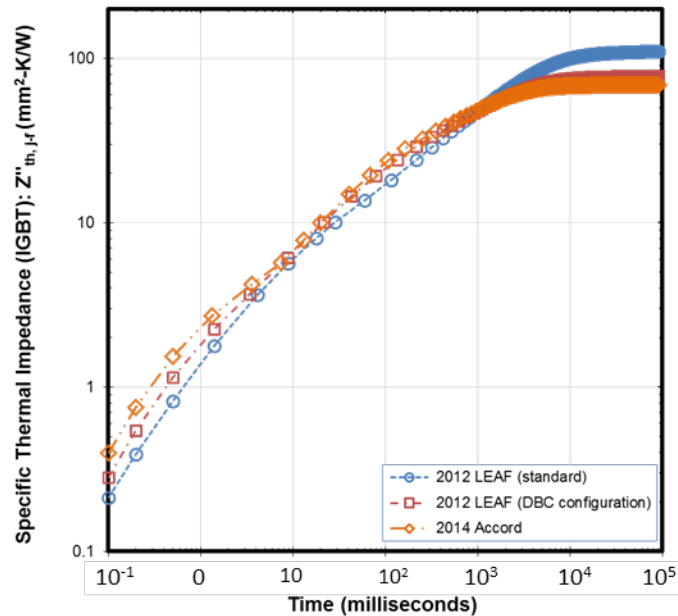


Figure I-7: Transient junction-to-liquid thermal impedance plotted versus time.

2015 BMW i3 power electronics (inverter) thermal management system

Benchmarking of the 2015 BMW i3 power electronics thermal management system also started in 2016. Figure 8 shows the images of the 2015 BMW i3 electrical machine electronics (EME), which serves as control electronics for the electrical machine. The electrical machine electronics fulfill the task of converting the DC voltage from the high-voltage battery into a three-phase AC voltage for operating the electric motor. It can also work as an alternator to convert the three-phase AC voltage from the electrical machine to a DC voltage to charge the high-voltage battery. Figure 8 also shows the cold plate and the drive board mounted on the power module. The power block is an Infineon HybridPACK 2 which was developed for hybrid-and electric vehicles. This module accommodates a three-phase six-pack configuration of Trench-Field-Stop IGBT 3 and matching emitter- controlled diodes, as shown in the right image in Figure 6. The power module also comes with an integrated pin-fin baseplate for direct cooling that significantly enhances heat removal from the chips. The cross-section view of the stack structure of the power module is shown in Figure 9. Detailed investigation of each layer's thermal property is in progress.



Figure I-8: Pictures of the 2015 BMW i3 inverter. The left image is the top view of the i3 EME system. The middle image shows the cold plate cooling channels. The image on the right shows the power block mounted on the cold plate.

Photo Credit: Xuhui Feng (NREL)

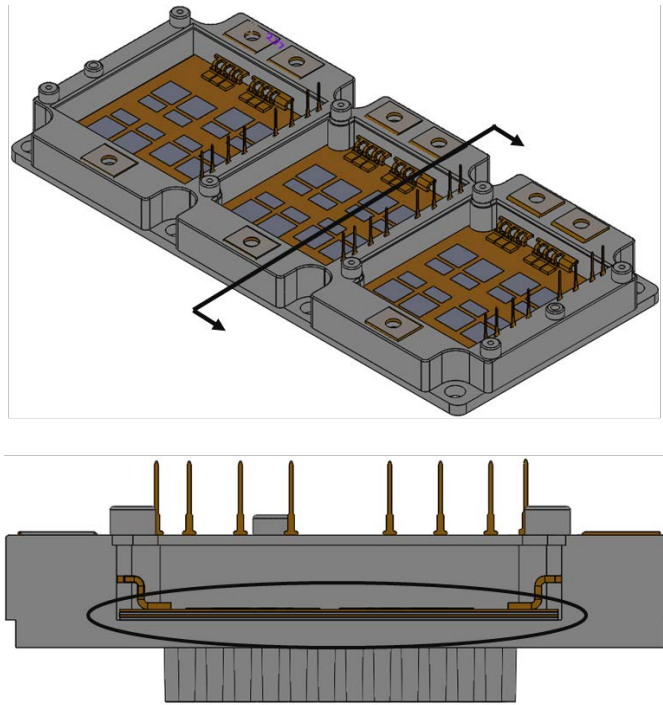


Figure I-9: CAD model of the BMW i3 power module (top). The various power module layers are circled out in the lower cross-section view.

Following the procedure adopted for the Accord power electronics, measurements of thermal resistance were also performed for the BMW i3 IGBT module. Figure 10 displays the junction-to-liquid thermal resistance versus various flow rates for the BMW i3 power module, along with that of the 2012 LEAF and 2014 Accord power modules. Experiments were conducted at flow rate, temperature, and input power values similar to those used for the Leaf and Honda power electronics systems. The BMW i3 system provided the thermal resistance in the range of 12–14 mm²·K/W, lower than the values from both the Leaf and Honda systems. At 12 Lpm, the i3 power module has a low junction-to-liquid thermal resistance of only 12 mm²·K/W, compared to 78 mm²·K/W for the LEAF and 42 mm²·K/W for the Accord. A possible reason for the significant improvement in the i3's specific thermal resistance is that the module incorporates higher thermally conductive materials and reduces the IGBT size. In-depth study of the materials and the properties within the stack module needs to be conducted to better understand the improved thermal performance. In addition, the junction-to-liquid thermal resistance shows minimal variation with the flow rates, suggesting that the stack thermal resistance is significantly larger than the convective resistance (at the flow rates tested).

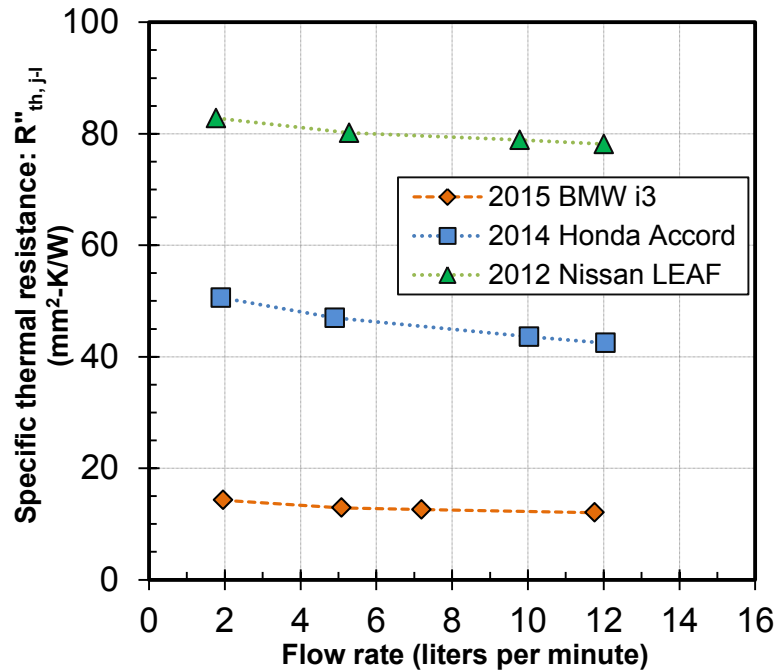


Figure I-10: Specific (junction-to-liquid) thermal resistance plotted versus the convective thermal resistance for the 2012 LEAF, 2014 Accord and 2015 BMW i3 power electronics systems.

Conclusions and Future Directions

In FY16, we benchmarked the thermal performance of the 2014 Honda Accord Hybrid power electronics thermal management systems. Both experiments and numerical simulation were utilized to thoroughly study the thermal resistances and temperature distribution in the power module.

- Experimental results obtained from the WEG tests provided the junction-to-liquid thermal resistance. The FEA and CFD models were found to yield a good match with experimental results. Both experimental and modeling results demonstrate that the passive stack is the dominant thermal resistance for both the motor and power electronics systems.
- The 2014 Accord power electronics systems yield steady-state thermal resistance values around 42–50 mm²·K/W, depending on the flow rates. At a typical flow rate of 10 Lpm, the thermal resistance of the Accord system was found to be about 44% lower than that of the 2012 Nissan LEAF system that was benchmarked in FY15. The main reason for the difference is that the Accord power module utilizes a metalized-ceramic substrate and the TIM layers are eliminated in the Accord module.
- FEA models were developed to study the transient performance of 2012 Nissan LEAF, 2014 Accord and two other systems that incorporate a conventional power module design. The simulation results indicate that the 2012 LEAF power module has lowest thermal impedance at a time scale less than one second. This is probably due to the moving of low thermally-conductive materials further away from the heat source and enhancement of the heat spreading effect from the copper-molybdenum plate close to the IGBTs. When approaching steady-state, the Honda system shows lower thermal impedance.
- Thermal Measurement results from the 2015 BMW i3 power electronic system indicate that the i3 IGBT module has significantly lower junction-to-liquid thermal resistance as compared to the other systems. At a flow rate of 12 Lpm, the thermal resistance of the i3 system is only 30% of the Accord system and 15% of the LEAF system.

Nomenclature

A	area
k	thermal conductivity

Q	heat
R th	specific thermal resistance
Z th	thermal impedance
T	temperature

Subscripts

j	junction
l	liquid

FY 2016 Presentations/Publications/Patents

1. Moreno, G., Bennion, K., King, C., and Narumanchi, S. "Evaluation of Performance and Opportunities for Improvements in Automotive Power Electronics Systems." The Intersociety Conference on Thermal and Thermomechanical Phenomena in Electronic Systems, Las Vegas, Nevada, May 2016.
2. Feng, X., Moreno, G., and Bennion, K. "Thermal Performance Benchmarking." 2016 DOE VTO Annual Merit Review, Washington, D.C., June 2016.

Acknowledgments

The author would like to acknowledge the support provided by Susan Rogers, Technology Development Manager for the EDT Program, Vehicle Technologies Office, U.S. Department of Energy Office of Energy Efficiency and Renewable Energy. The significant contributions of Gilbert Moreno and Kevin Bennion are acknowledged.

References

1. Burress, T. "Benchmarking of Competitive Technologies." 2012. DOE VTO Annual Merit Review, Washington D.C., May 2012.
2. Burress, T. "Benchmarking EV and HEV Technologies." 2015. DOE VTO Annual Merit Review, Crystal City, VA, June 2015.
3. Burress, T. "Benchmarking EV and HEV Technologies." Oak Ridge National Laboratory, 2014 VTO EDT Annual Report, 2014.
4. Lau, J. H., and Pao, Y. "Solder Joint Reliability of BGA, CSP, Flip Chip, and Fine Pitch SMT Assemblies, 1997." NY McGraw-Hill.
5. MatWeb. "CeramTec SL200B Silicon Nitride." <http://www.matweb.com/search/DataSheet.aspx?MatGUID=50f707073d0149218469a887fb0bbf31>.
6. MatWeb. "Aleris 55HX Aluminum (5005-h14)." <http://www.matweb.com/search/DataSheet.aspx?MatGUID=b8de580814574dda958c8b2a4aeb710>.
7. MatWeb. "Overview of Materials for Polyphenylene Sulfide (PPS) with 40% Glass Fiber Filler." <http://www.matweb.com/search/datasheet.aspx?matguid=301e3f904d6a43a7922601c9d11ded91>
8. Bennion, K., and Moreno, G. "Thermal Management of Power Semiconductor Packages-Matching Cooling Technology with Packaging Technologies." Second Advanced Technology Workshop on Automotive Microelectronics and Packaging, Dearborn, MI, April 2010.